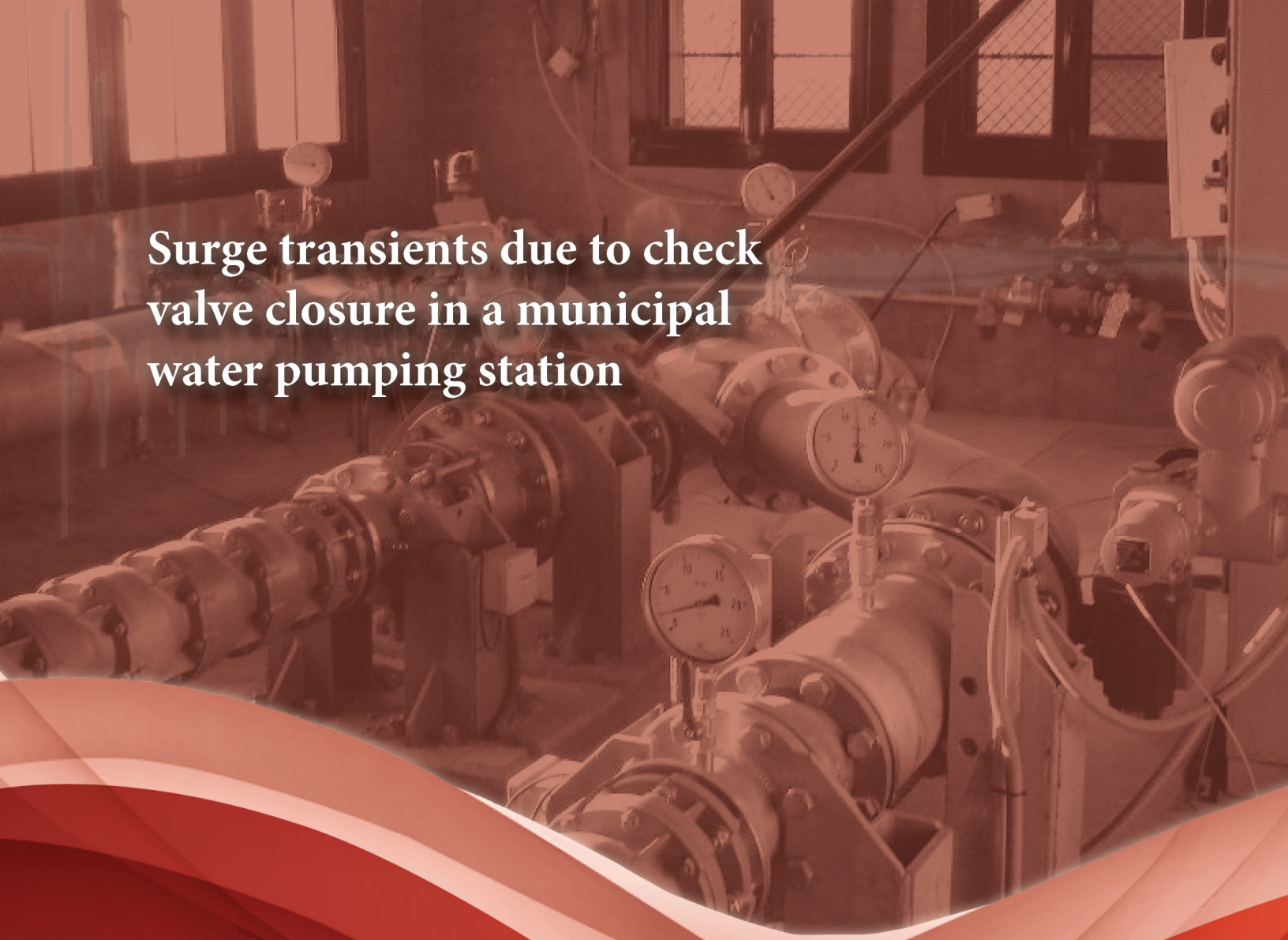

Surge transients due to check valve closure in a municipal water pumping station

D Lozano Solé
R Bosch Segarra
Aquatec Proyectos para el Sector del Agua SAU (SUEZ Group), Spain

Trey Walters P.E.
Applied Flow Technology
Colorado Springs, Colorado, USA

13th International Conference on
Pressure Surges 2018
Bordeaux, France, 14th-16th November 2018

Surge transients due to check valve closure in a municipal water pumping station

D Lozano Solé[1], R Bosch Segarra[1], T W Walters[2]
[1] Aquatec Proyectos para el Sector del Agua SAU (SUEZ Group), Spain
[2] Applied Flow Technology, USA

ABSTRACT

The present study highlights the importance of proper check valve selection to mitigate waterhammer and its associated problems. Two different check valves were installed in a pumping station in a municipal water transfer system: a swing check valve and a nozzle check valve. Measurements were taken of pipeline pressures after a pump trip and resulting check valve closure. The field data was compared to predictions from a model using a commercial waterhammer tool. Commonly accepted methods for estimating reverse liquid velocity at check valve closure were utilized. Results were also compared to previous experimental test from other authors. The calibrated model results matched the field data quite well. Comparisons of inferred valve characteristics to previously published results for swing and nozzle valves were not in close agreement for either tested valve.

ABBREVIATIONS

DGCM	Discrete Gas Cavity Model
HFPT	High Frequency Pressure Transducer
MOC	Method of Characteristics
PS	Pump Station

1 INTRODUCTION

Water supply systems are strategic infrastructures that guarantee the welfare of the population and ensure the country's economic development. This means that water utilities must ensure the continuity of supply, the quality and the service pressure at all time. To meet this goal Asset Management Plans have to be implemented to maintain a desired level of service at the lowest life cycle cost. As part of these plans, renewing and replacing system components are essential activities. Pumping stations are strategic assets in water distribution networks and these activities have a direct impact on them.

When design engineers are faced with a pumping station in need of revamping, they are challenged to size and specify new mechanical equipment at the lowest budget while maintaining the system's operational conditions. The task becomes more complicated when tackling transient analyses with (frequently) limited information available about the existing system. Engineers are thus compelled to hypothesize and make assumptions. The renewed system should perform in such a way that surge pressures reached during

operations are at similar or even lower values than the current ones. It has been widely demonstrated by water operators that the origin of burst mains is frequently a result of unexpected and rapid pressure variations, especially in periods of low water consumption in which energy dissipation potential is reduced.

With this in mind, the solution lies in a proper choice of protection devices (e.g., surge vessels, relief valves, surge tanks). Equally important is proper check valve selection, as this is often the origin of the pressure surge. Regarding protection devices, extensive information of their features and performance is supplied by manufactures or available in the catalogue. On the other hand, limited information is traditionally provided by check valve suppliers related to its dynamic performance despite its direct relationship to waterhammer. Manufacturers don't usually provide this information because the hydraulic conditions of the system affect the check valve performance. That means that they need to test their valves under a wide range of scenarios to determine the closing time or the expected reverse velocity. Because of this lack of information, the issue has been extensively studied in research projects where tests have been performed under well-controlled conditions (this will be discussed further in Section 2). These documented experiences provide surge modellers with approximate information about the dynamic performance of check valves.

The system studied in this paper had one operating pump and one standby pump. It also had a surge vessel at the pump discharge side. Thus the check valve slam was driven by gravity and the surge vessel, and not by parallel pump trip and operation.

With the goal of illustrating check valve slam in an installed system and the difficulties modellers encounter when performing transient analyses, the authors present a case study carried out on a recently refurbished pumping station in the Barcelona distribution network. The water operator, aware of the impact of check valves on surge pressure, decided to install two different check valves to compare the pressures reached during a pump trip event. A detailed hydraulic model of the system was developed with the commercial software AFT Impulse (Applied Flow Technology, 2016 (1)) and the results were compared with field data gathered by the SCADA and a high frequency pressure transducer expressly installed for the test.

The goals of the present case study are:

- Compare the slamming effect of two different check valves: a conventional swing check valve vs. a nozzle check valve.
- Reinforce the importance of proper check valve selection.
- Discuss the importance of energy dissipation during a transient event on complex systems.
- Explore agreement between computed and measured pressures during a transient event.
- Improve understanding of the robustness and reliability of computational modelling tools based on the MOC to perform transient analyses.

2 REVIEW OF CHECK VALVE RESEARCH

The slam phenomena associated with check valve closure has been widely studied due to its undesirable effects and its potential damaging consequences:

Effects	Potential damaging consequences
Pressure exceeding maximum allowable pressure	Stress on pipes Pipe burst risk
Damage on check valve seat / body	Leakage of water from outlet side to inlet side High pressure from the outlet side can be transferred to the inlet side exceeding rated pressure of pipes and equipment Pipe burst risk
Vibration	Movement of equipment Need for additional restraints Leakage of water
Noise	Disturbance to operators and population

Check valve suppliers, aware of the slam effect and its consequences, have developed two strategies to improve the dynamic features of their valves:

- Ensuring a very fast closure to minimize as much as possible the reverse flow after planned or unplanned pump shut down
- Ensuring a very slow closure once the reverse flow takes place after planned or unplanned pump shut down

The understanding of closing check valves during waterhammer events has significantly evolved over the last four decades. While many uncertainties remain, accepted methodologies for simulating check valve closure are now available. Two different approaches have evolved. The first is a physics-based approach where a force or torque balance on the valve is performed. The second is an empirical approach whereby valve characteristics are either independently tested or, more frequently, estimated from valves of similar design. See References (2-8).

Of great significance is the identification of what appear to be two important parameters that impact check valve closure. These are the 1) reverse fluid velocity at valve closure and, 2) the valve deceleration (often observed to be mostly linear). With these parameters, charts are available in either dimensional or dimensionless form for various types of check valves. The charts by Thorley (5-6), Valmatic (7) and Ballun (8) are commonly used (note that References 7 and 8 are related). These charts will be discussed later in this paper as part of the results presentation.

Liou and Li, 2004 (9) present experimental check valve closure data and an improved torque balance calculation method. This calculation method is not available in the simulation software used in this study (1). Adriasola and Rodríguez, 2014 (10) present an index for classifying severity of check valve slam during pump trips among parallel pumps in operation. The current study does not operate parallel pumps hence this is not relevant here. Marcinkiewicz et al., 2014 (11) offer additional experimental results of check valve closure.

3 CASE STUDY

3.1 System features

The present transient study was carried out in a pumping station in the Barcelona water distribution network. The huge network operated by Aigües de Barcelona (Suez Group) serves water to 3.2 million people in 23 municipalities. Due to local orography, the network is divided into several pressure sectors to optimize the energy consumption. The project

took place in the Tibidabo Pumping Station (hereinafter referred to as Tibidabo PS), which supplies water to the highest neighbourhood of Barcelona, known as Vallvidrera. Due to inefficient operation and the fact the equipment had exceeded its design life, all mechanical, electrical and ICA equipment was replaced in 2016.

Tibidabo PS transfers water from Sant Pere Martir tank, at 300 m above sea level, to Vallvidrera tank, at 437 m above sea level. The pumping station, at 280 m above sea level, is located 3.100 m away from the Sant Pere Martir tank and connected by a DN 300 mm ductile iron main. This main also has several connections that serve water to other secondary networks on its route.

The Tibidabo PS (Figure 1) is equipped with 2 new INDAR well pumps mounted "horizontal in jacket" to reduce the noise impact outside. The model installed is a UGP – 1030/7 (7 stages), with a capacity of 0,080 m^3/s at 155 m (duty point) and 220 kW (400V – 50 Hz), rotating at 2.900 rpm, operating one as duty and the other as standby. The revamping also involved increasing the capacity of the old pumps that were transferring up to 0,060 m^3/s to Vallvidrera tank.

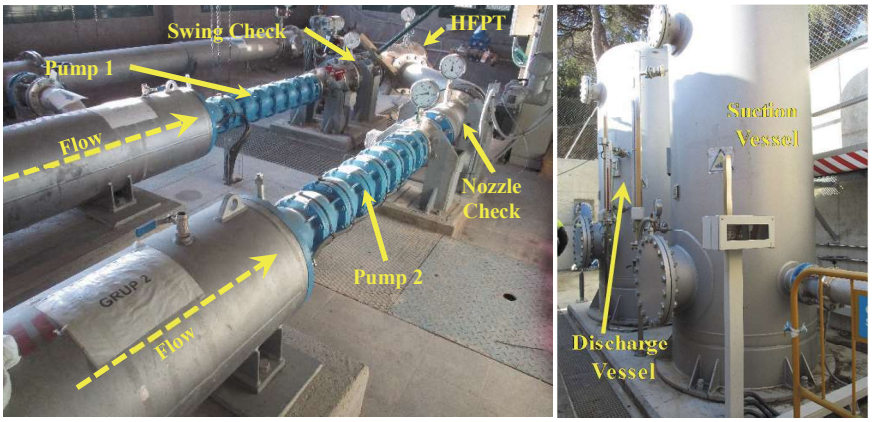

Figure 1. Pictures of the pump sets and the surge vessels (pump suction/discharge) installed at Tibidabo PS.

All pipework inside the building is made of stainless steel; 12'' for common manifolds (suction/pressure side) and 8" for each pump set branch. Outside Tibidabo PS, the pumping line has a length of 1.338 m, composed by 485 m of an old DN 300 mm reinforced concrete cylinder pipe laid in 1977, and 853 m of DN 300 mm K9 ductile iron pipe with a maximum allowable operating pressure of 49 bar. The rated pressure of the concrete pipe is unknown and its maximum allowable pressure has been determined by the rated pressure of the old surge vessel, 20 bar. This value is consistent with the commercial maximum pressure of this type of pipe, around 300-400 psi (20–27 bar). The main has also two connections that serve water to two small consumers. Additionally, there is a DN 200 ductile iron connection branch to a higher-pressure sector (Tibidabo-Torreó water tank, at 512 m above sea level) that remains closed during normal operation and allows water transfer in case of emergency. The position of the isolating valve, at elevation 452 m, creates an air pocket inside the DN 200 connection branch, as the water level in Vallvidrera tank is at 437 m. The estimated volume of the air content is 0,628 m^3. Figure 2 shows a schema of the system described.

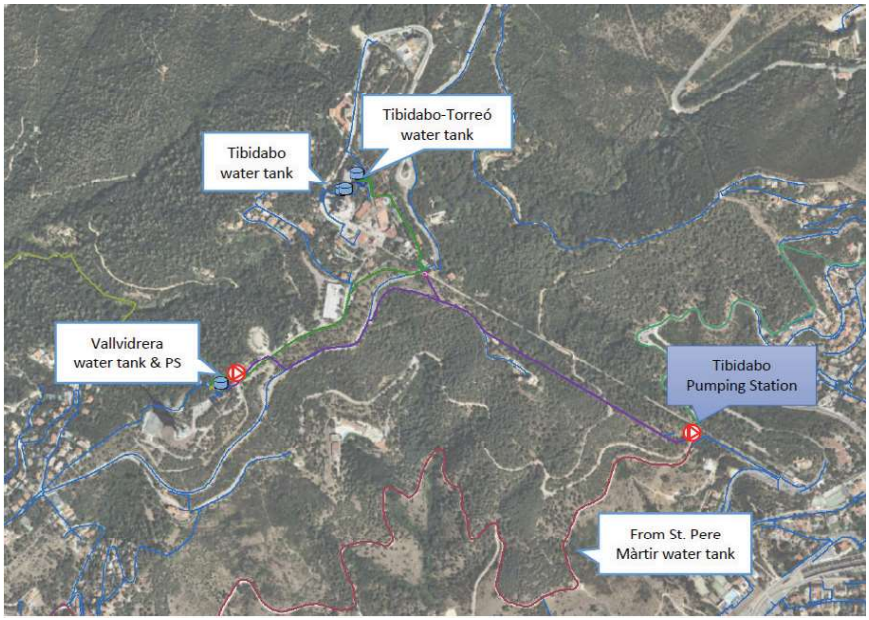

Figure 2. General overview of the Tibidabo water pumping system.

To protect the suction pipe against pressure surges, a 4,29 m^3 surge vessel has been installed. It has an initial air volume of 1,66 m^3 (pumps not running). At the outlet side, a 6,18 m^3 surge vessel with an initial air volume of 3,41 m^3 protects the pumping line. See Figure 1, right. Both surge vessels are made of carbon steel with no bladder. The air volume is controlled through the SCADA and the compressor installed on the premises. The initial air volumes recorded by the SCADA during the test for the inlet and outlet surge vessels were 2,22 m^3 and 3,40 m^3 (steady state), respectively.

Data regarding the maximum pressure raised prior to the revamping is not available since the installation of the new PLC in 2016. The rated pressure obtained from the old surge vessel data-plate, 20 bar, has been used as reference of maximum allowable pressure of the pumping line. The safety valve installed on the surge vessel was also set at 20 bar.

3.2 Tested check valves

As mentioned, the pump sets are equipped with two different check valves: one with a conventional swing check and the other one with a nozzle check. Previous transient analyses performed on other pumping stations in the Barcelona network highlighted the need to measure the real impact of traditionally installed check valves. Swing check valves have been widely used for several reasons:

- Traditional design habits adopted by engineers (commonly accepted past practice).
- Maintenance standardization consequences. Operators tend to standardize and reduce variability simplifying the maintenance and replacement. These principles sometimes go against optimal hydraulic solutions.
- Mechanical and operational simplicity. Swing check valves are preferred by O&M staff instead of better check valves (in terms of dynamic performance). The lower number of moving parts in the check valve, the less risk of failure and maintenance.
- Low purchase price.

- Installation low lying length, especially compared to check valves with motion assist mechanisms (oil cylinders).
- Necessity of better understanding of check valves dynamic performance and different types of check valves available in the market.
- Misunderstanding about the surge vessel protection capacity. Surge vessels are known as excellent devices to protect systems against surge pressures, maximum and minimum, but they are not able to avoid the slam from the check valve when it closes instantly (or not at all).

Regarding the swing check valve, a DN 200 model ZRK 3 from Rittag is installed downstream of Pump 1. Both the body and the disc are made of stainless steel. Technical brochures from the supplier only provide information about materials, dimensions and head losses. Figure 4 shows the valve installed at Tibidabo PS and general valve data.

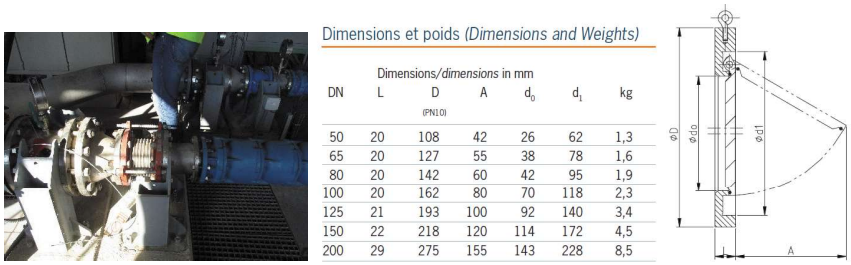

Dimensions et poids *(Dimensions and Weights)*

Dimensions/*dimensions* in mm

DN	L	D (PN10)	A	d_0	d_1	kg
50	20	108	42	26	62	1,3
65	20	127	55	38	78	1,6
80	20	142	60	42	95	1,9
100	20	162	80	70	118	2,3
125	21	193	100	92	140	3,4
150	22	218	120	114	172	4,5
200	29	275	155	143	228	8,5

Figure 3. Swing check valve installed on Pump 1 and main features from the manufacturer's technical brochure (Rittag).

On the other hand, Pump 2 has a DN 150 non-slam nozzle check valve from Erhard, with the body made of ductile iron and disc of rubber coated bronze. The nozzle check has an internal spring that ensures a fast closing. In this case, apart from the common technical data, the brochure contains additional information regarding the dynamic performance of the valve. The following chart (Figure 4) from Erhard (12) provides approximate information about the expected reverse velocity at closure vs. the flow deceleration. Note that installed pipe downstream of this valve is DN 200, and thus a DN150 to DN200 expansion fitting was installed just downstream of the nozzle check valve. The effect of this diameter change and, hence, velocity change when flow is reversing and the valve is closing is unknown by the authors.

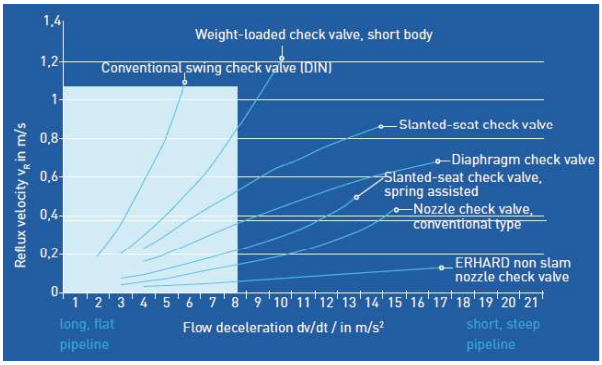

Figure 4. Nozzle check valve (section) installed on Pump 2 and dynamic information from the manufacturer (Erhard). From Erhard Technical Brochure (12).

The chart shows similar information to the ones provided by field tests carried out by Thorley (4-6) and Ballun (8).

3.3 Field test performed and data collection

The first part of the survey consisted of recording the surge pressure caused by stopping the installed pump sets, running separately. The stop order from the panel control took place when the butterfly valve downstream of the pumps was 40% open. As high vibration was experienced in the trip off tests during the commissioning phase, the facility owner operator wanted to avoid a fully open valve position. The authors thus had no control over this decision by the facility owner. Certainly, while the optimal test would be done with the outlet valve 100% open, it is not believed that created a significant impact on the results as butterfly valves are known to only cause significant flow reductions when they are almost closed. No variable speed drives are installed and soft starters control starting/stopping sequences. The two pump trips (between the swing and nozzle check tests) were separated by 20 minutes and the stop order took place when pressures were steady. The test was carried out in January 2017.

The survey involved recording several performance variables that were obtained from the SCADA: pressure inlet/outlet side, flow, valve position downstream of the pumps and air level in the surge vessels (inlet/outlet). Additionally, to record the expected rapid pressure variation, a high frequency pressure transducer (hereafter HFPT) was installed downstream of the check valves. The measurements were recorded by a Multilog from HMW, a pressure transducer–datalogger specially designed to record fast transients and able to log up to 25 measurements per second.

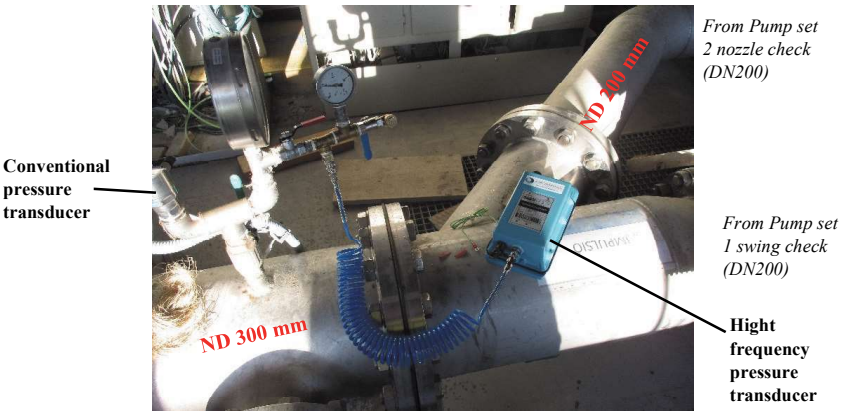

Figure 5. The picture shows the Multilog installed on the outlet side, next to the existing pressure transducer (outlet PIT on the left).

The pressure on the SCADA was recorded by a conventional pressure transducer (hereinafter CPT) from IFM (model PN2023). The CPT was set to refresh pressure values to the SCADA up to 10 times per second.

The second part of the study consisted of modelling the system with a commercial simulation tool to check the reliability of the numerical model and to determine difficulties and constraints for modelling real systems like Tibidabo PS.

4 NUMERICAL MODEL AND SIMULATION TOOL

The simulation tool used in this study, AFT Impulse, is commercially available (1). It employs the method of characteristics (MOC) to solve the governing equations (13, 14). It has a built-in steady-state solver to initialize the transient which is independent of the MOC. It has check valve models based on Thorley (6) as well as a swing check valve torque balance model from Wylie and Streeter (13). Because reverse velocity occurs through the check valve, reverse flow through the pump occurs for short time periods and a four-quadrant pump trip model was accessed in the software. Once the check valve closed, the pump was isolated from the piping downstream of the check valve and the pump model no longer mattered.

The software does not include frequency dependent friction models or effects from fluid-structure interaction (FSI). As FSI was not modeled, the vibration effect on the system pressure response was not accounted for.

The software does not include a model for air release. It does include modelling of transient cavitation. In the swing check valve simulation minor transient cavitation was predicted. Peak vapor volumes of 0.75 liters (2% of computing volume) were predicted between the pump and check valve after the valve closed. These thus had no impact on the simulation downstream of the check valve as it was closed by this time. About 700 m downstream of the check valve local vapor was generated with a maximum volume of 0.02% of computing volume. The Discrete Gas Cavity Model (DGCM) (13, 15) was used for this simulation. This local vapor formation identified by the model occurred 70 m upstream the DN 200 connection branch to Tibidabo-Torreo water tank (see Figure 6, gas accumulator #13, pipe element #16). It occurs 0.5-1 seconds after the check valve closed and thus has no impact on the largest pressure spikes in the results shown in Section 5. It only lasted for a short time. For this reason and for space limitations, results are not shown for the cavitation. This reasons for the low pressure and predicted cavitation at this location is explained by the following facts:

- The pipe profile turns flat from 600 m downstream of the PS to the Vallvidrera tank and the minimum hydraulic gradeline is close to the pipe elevation profile
- The DN200 connection, performing as a surge vessel due to the air pocket content, is fully emptied which makes the pressure fall below 0 just upstream.

The small volumes computed and the short section affected are not considered a significant risk of causing damage to the ductile iron main.

The model implemented was initially calibrated on the steady state by using the data provided by the SCADA and the roughness friction was slightly adjusted to get the best agreement.

Figure 6 shows the Tibidabo PS model diagram.

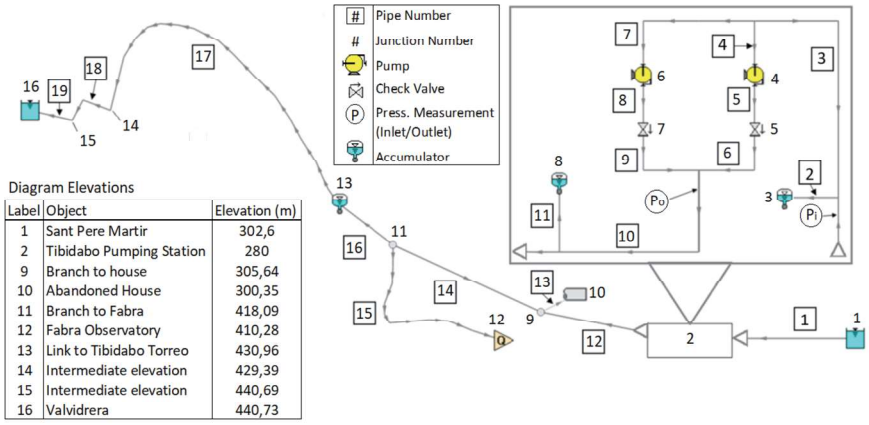

Label	Object	Elevation (m)
1	Sant Pere Martir	302,6
2	Tibidabo Pumping Station	280
9	Branch to house	305,64
10	Abandoned House	300,35
11	Branch to Fabra	418,09
12	Fabra Observatory	410,28
13	Link to Tibidabo Torreo	430,96
14	Intermediate elevation	429,39
15	Intermediate elevation	440,69
16	Valvidrera	440,73

Figure 6. Model diagram implemented using Reference (1).

Main data from the model is listed below in the following tables:

Pipe	Length (m)	Diameter (mm)	Material	Roughness (mm)	Wavespeed (m/s)
1	3100	304,8	Stainless steel	0,046	1246
12	67,1	300	Concrete	3,5	1113
13	26	33,4	HDPE	0,0015	373
14	200	300	Concrete	3,5	1113
	217,9	300	Concrete	3,5	1113
	76,7	328,8	DI	5	1074
15	171,5	106,8	HDPE	0,0015	374
16	130,9	328,8	DI	5	1074
17	457,2	328,8	DI	5	1074
18	151,4	328,8	DI	5	1074
19	36,5	328,8	DI	5	1074
2	10	202,72	Stainless steel	0,046	1277
3	5	304,8	Stainless steel	0,046	1246
4	5	202,72	Stainless steel	0,046	1277
5	2,5	202,72	Stainless steel	0,046	1277
6	2,5	202,72	Stainless steel	0,046	1277
7	5	202,72	Stainless steel	0,046	1277
8	5	202,72	Stainless steel	0,046	1277
9	5	202,72	Stainless steel	0,046	1277
10	10	304,8	Stainless steel	0,046	1246
11	5	202,72	Stainless steel	0,046	1277

Inlet Gas Accumulator	
Number	3
Polytropic Constant	1.2
Gas Volume - Steady State	2.22 m^3

Outlet Gas Accumulator	
Number	8
Polytropic Constant	1.2
Gas Volume - Steady State	3.40 m^3

Pumps	
Number	4,6
Four quadrant data set	Ns = 0.46
Rated Pump Speed	2900 rpm
Rotating inertia	1.59 $kg*m^2$

Swing Check Valve	
Number	5
Forward Velocity	-0.92 m/s
Fully Open Cv	1445
Set to not re-open	

Nozzle Check Valve	
Number	7
Forward Velocity	-0.15 m/s
Fully Open Cv	400
Set to not re-open	

5 RESULTS AND DISCUSSION

5.1 Check valve performance under transient conditions

Figure 7 compares the slam effect as measured for both swing and nozzle check valves. The comparison has been done with data provided by the HFPT at the DN300 pipe in Figure 5. Results clearly indicate that the swing check valve causes significantly higher pressures when closing, recording 47 m above the steady state. On the other side, the nozzle check valve raises the pressure about 8 m above the steady conditions when closing. The poorer performance of the swing check valve, in terms of slam, causes 83,3 m of max/min pressure variation in less than a second (217,7 – 134,4 m), as shown in Figure 7.

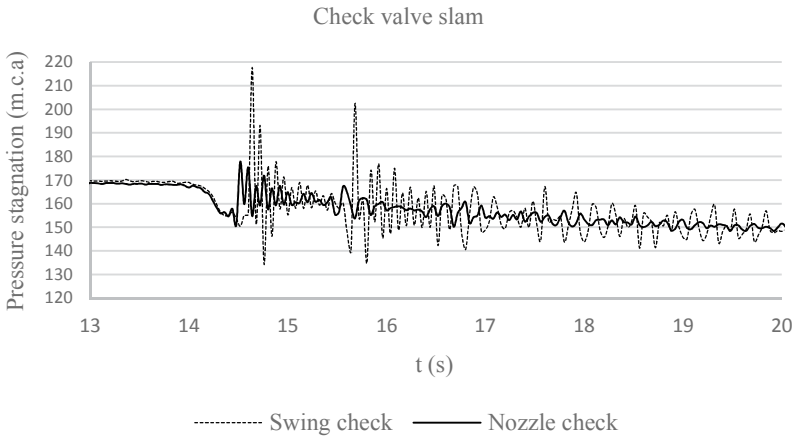

Figure 7. Transient pressures comparison between both check valves. Pressure values recorded by HFPT.

As mentioned in the experimental test of several check valves performed by Valmatic (7), the considerable inertia of the disc, its long travel to close and the lack of a spring to assist the motion are the primary reasons the larger slam occurred.

The check valve slam comparison highlights the importance of a proper check valve selection with a fast closing when the trip takes place. The first and second peak pressures caused by the swing check valve slam (217,7 and 202,4 m) exceed instantly the maximum allowable pressure on the system, 20 bar (200 m), determined by the old surge vessel data-plate. On the other, the peak pressure with the nozzle check (177,8 m) is lower than the maximum pressure set before the pumping station revamping.

Other accepted strategies to reduce the slam consist of installing assisted check valves with oil cylinders. These types of valves commonly have 2 or 3 closing stages, closing fast at the beginning and ensuring a slow closure at the end of disc motion when reverse velocity occurs. Several suppliers provide this type of valve such A.R.I. (HCCV Full Hydraulic Transient Control) and DeZurik (APCO CVS6000). The use of these check valves is complex and design engineers must properly study both the check valve and the pump because that will experience reverse rotation and this could damage mechanical parts (seals, coupling, motor, etc.). Despite the benefits of these assisted check valves in terms of slam, they are not widely used among water operators for the following reasons:

- More expensive than other types like swing check or nozzle check valves.
- More complex operation and maintenance because of the hydraulic operation. Water operators look for simple and robust systems with few moving parts that can fail.
- Bigger lying lengths requirements. Revamping an old pumping station requires that all new equipment fit in places where lack of space is traditionally a common issue.
- Water operators tend to standardize their equipment and introducing new alternatives is not easy, especially if they are more expensive and more complex.

5.2 Comparison between modelled and measured pressure

The last part of the test compares the model, based on the MOC, with the field data gathered with the SCADA and the HFPT. Initially the model was calibrated for steady-state with all data available from SCADA. The only component of the system that required an additional calibration process on the transient scenario was the check valve. As mentioned, a four-quadrant trip model was accessed and reverse velocity on the check valve was required. Several reverse velocities have been assessed until getting the best agreement with the values recorded by the HFPT. The model has been matched for the maximum peak pressure recorded by the HFPT.

Additionally, Thorley and Ballun values were also implemented considering deceleration values from the model (7,23 m/s^2 for swing check and 6,59 m/s^2 for nozzle check). The following Table 1 shows the pressure comparison for the instant slam with all velocity references used. The pressure comparison is referenced to the section where the HFPT was installed, shown in Figure 5.

Table 1. Summary of peak pressures after check valve slam using various models and methods.

Check valve	**Reverse velocity at check valve, DN200, (m/s)**	**Pressure - slam instant (m) at DN300 HFPT location** *Pressure variation referred to HFPT in parentheses*	
		Maximum	**Minimum**
Swing check (Pump 1)	*HFPT (field data)*	*217,7*	*134,4*
	1,7 (Thorley swing, DN100, Fig 10)	**262,7 * (-17%)**	**121,4 * (10,7%)**
	0,92 (model best agreement)	**218,5 (-0,4%)**	**144,9 (-7,3%)**
Nozzle check (Pump 2)	*HFPT (field data)*	*177,8*	*151,1*
	0,05 (Thorley strong nozzle, DN300, Fig. 10)	*173,6 * (+2,4%)*	*159,2 * (-5,1%)*
	0,15 (model best agreement)	**178,1 *(-0,2%)***	**158,9 *(-4,9%)***

** = pressure results from model using the referenced reverse velocity at check valve closure*

Regarding the swing check, Table 1 shows the reverse velocity in the model to get the best match with HFPT peak pressure is 0,92 m/s. This is considerably lower than the value obtained from Thorley DN100 curve (~1,7 m/s) with deceleration of 7,23 m/s^2 in Figure 8.

The nozzle check reverse velocity to get the best model match with the HFPT peak pressure is 0,15 m/s. The values from Thorley (DN300, strong nozzle, Figure 8) and the ones

announced on the supplier's brochure are lower (0,05 m/s). These show considerable scatter which is perhaps understandable considering the geometry and uncertainties as discussed earlier. Nevertheless, as the curves for all better dynamic performance valves are very similar, flat and weakly influenced by deceleration values, no major differences in terms pressure are observed from the Thorley model.

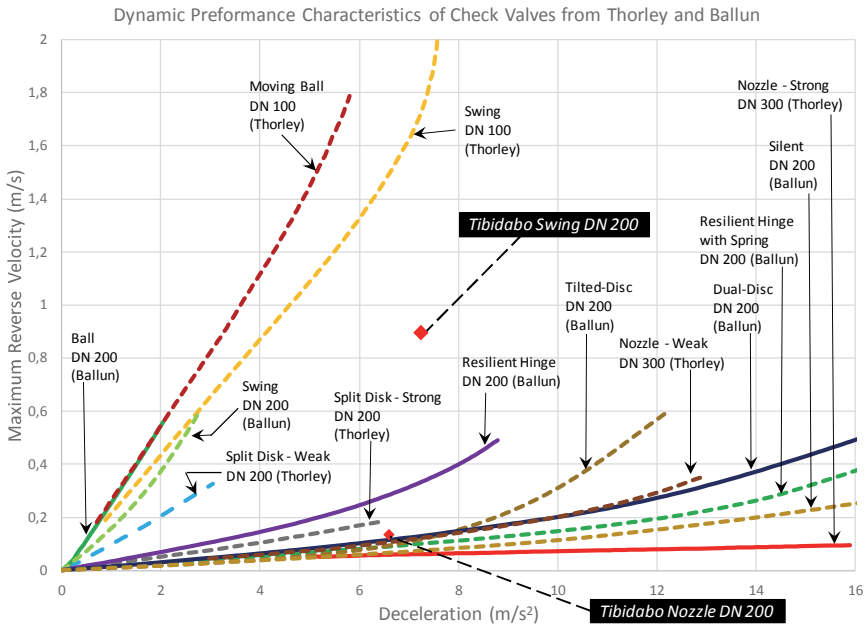

Figure 8. Dynamic performance of different check valves, from Thorley (6) and Ballun (8) experimental tests, along with estimated performance of Tibidabo installed valves (from Table 1).

Figures 9 and 10 compare the pressure values recorded with the HFPT and the ones modelled for the initial instant after the pump trip. As shown, the commercial tool model provides good agreement on the initial pressure oscillations.

The slight pressure head drop measured prior to the pump shut down (Figures 9 and 10, at <14 seconds) is explained by the partial closure of a manually operated butterfly valve downstream of the pump. The model does not show this effect because the position of the butterfly valve has not been considered in the modelling. This simplification does not impact the results due to the low effect of the butterfly valve when is still 40% open. During the pump trip transient the butterfly valve was left in at the 40% position.

On the other hand, both Figures 9 and 10 show significant differences between HFPT data and model regarding the pressure head drop during the initial stage of the shut down (t=14 s). Note that the model results shown in Figures 9 and 10 were calibrated to match the maximum pressures at roughly 14.5 seconds. Thus the valve reverse velocities used were those that matched the maximum. Not the minimum. See Table 1. A more perfect model would match both equally well. There are many reasons that could cause this discrepancy and it was not the purpose of this field study to research this. One obvious potential explanation is the relatively crude model used to represent the check valve. Another is the

local geometry of the DN300 tee where data was taken, the check valves in the DN200 pump discharge piping, and the nozzle check being itself DN150 as discussed earlier.

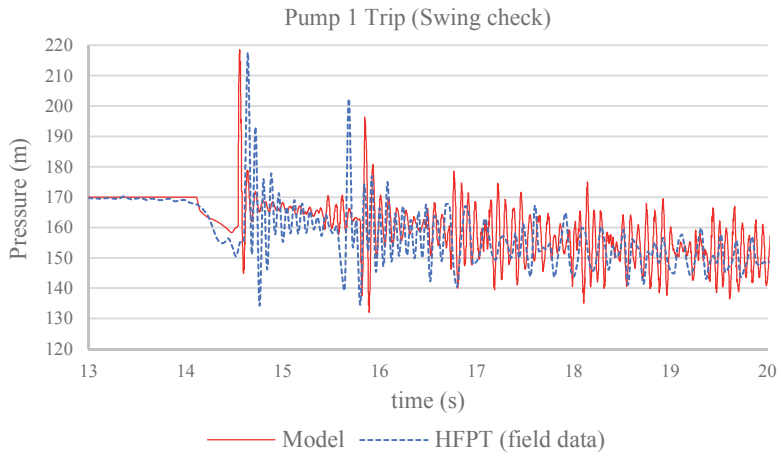

Figure 9. Modelled pressure at HFPT location *vs* recorded pressure oscillation for swing check pump set during the first seconds after the trip.

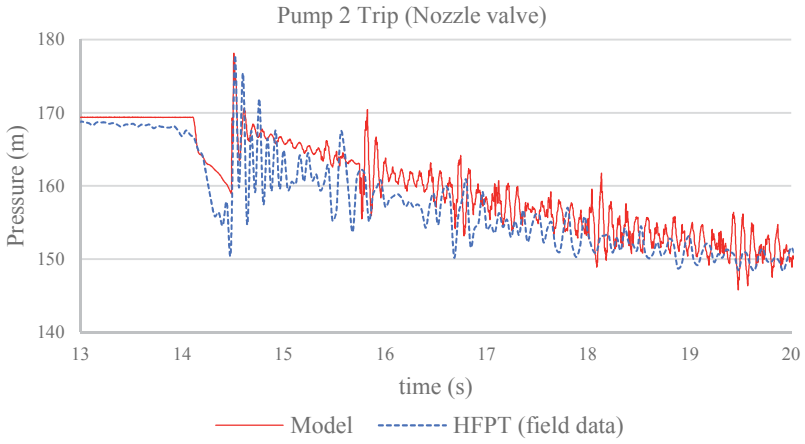

Figure 10. Modelled pressure at HFPT location vs. recorded pressure oscillation for nozzle check pump set during the first seconds after the trip. Note that the Y scale has been modified from Figure 9 to better show the comparison between the model and the HFPT data.

The correlation between modelled pressure values and recorded ones have been analysed for over 60 seconds after the pump trip. At this time (trip instant + 68 s), the pressure oscillation decay and the system tend to meet the static head. Figures 11 and 12 show this comparison for swing and nozzle check valves, respectively. In both graphs the model shows good agreement from the trip instant until 15 – 20 s after, when the system is less influenced by energy decay mechanisms. After 15-20 s until 68 s (time 80 s on Figures 11

and 12) the pressure variation shape is similar to the measured one from HFPT but 5 to 10 m of difference are observed.

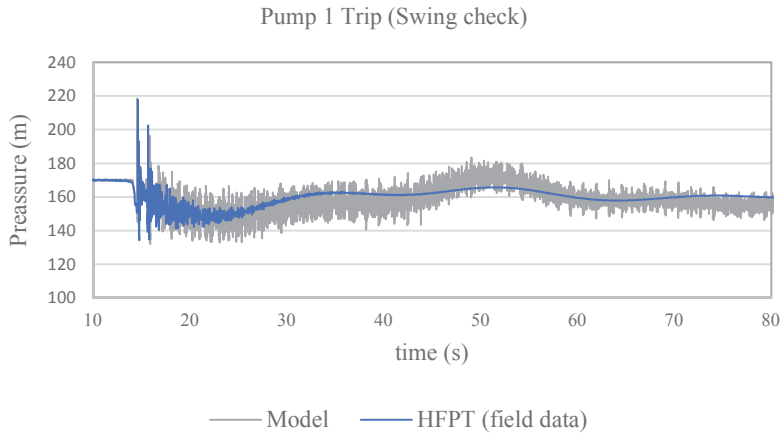

Figure 11. Modelled pressure vs. recorded pressure oscillation for swing check pump set during the minute after the trip.

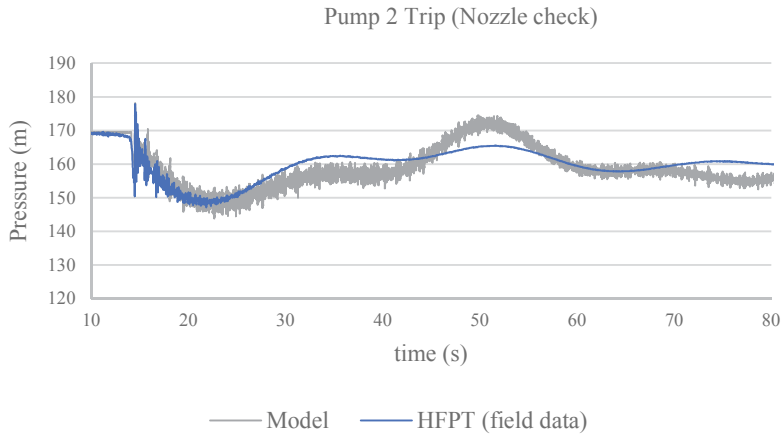

Figure 12. Modelled pressure vs. recorded pressure oscillation for nozzle check pump set during the minute after the trip.

According to Karney (16) the primary energy dissipation mechanism that would explain the differences observed on Tibidabo PS are the following ones:

- Unknown head losses from fittings and connections not covered on GIS data.
- Changes on consumption from the two existing connections on the main due to the experienced pressure change during the transient event. Slight increases in flow in response to the initial pressure peaks would be effective dissipative outlets for transient energy.
- Presence of leaks that would perform as changes on consumption (flow increase).

- Presence of additional branches, connections not in service and looped pipes not introduced on the model to simplify time calculation and model complexity.
- Unsteady friction. Under transient conditions, the rapid acceleration/deceleration of fluid can cause significant distortion of the velocity profile, and can thus cause much higher rates of energy dissipation or loss. Classic 1D models implemented on commercial transient tools use steady friction formulas to compute transient head losses. As Chaudry (14) indicates, these models yield satisfactory results for computing the first peak but show very slow dissipation pressure compared to measures on experimental test or real system such as Tibidabo PS case study. This author and many other such as Karney (16), Abreu (17) and Leite (18) have analysed the subject in recent decades and describe methods to provide more accurate simulations. Nevertheless, these sophisticated methods are not commonly used on commercial tools due to its complexity, being mostly used only on experimental and laboratory tests.

In addition to line pressure comparison, water level in the surge vessel (outlet side) has been also compared between SCADA data and the model showing similar agreement, Figures 13 and 14.

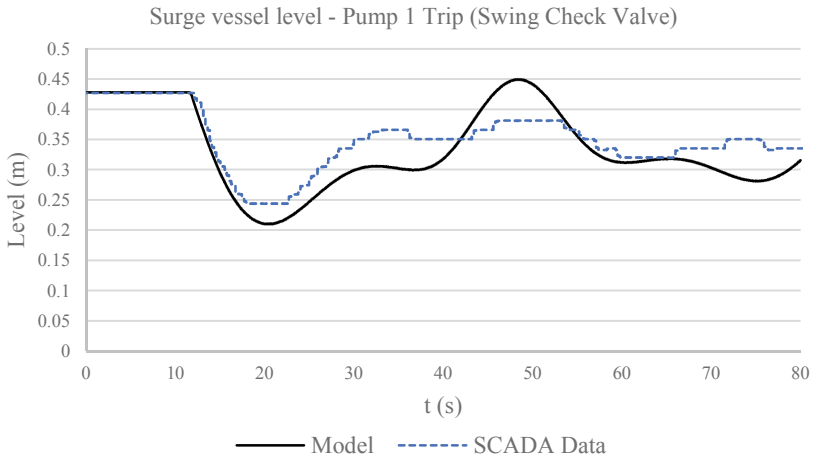

Figure 13. Modelled water level in the surge vessel vs. recorded level on the SCADA for swing check valve after trip.

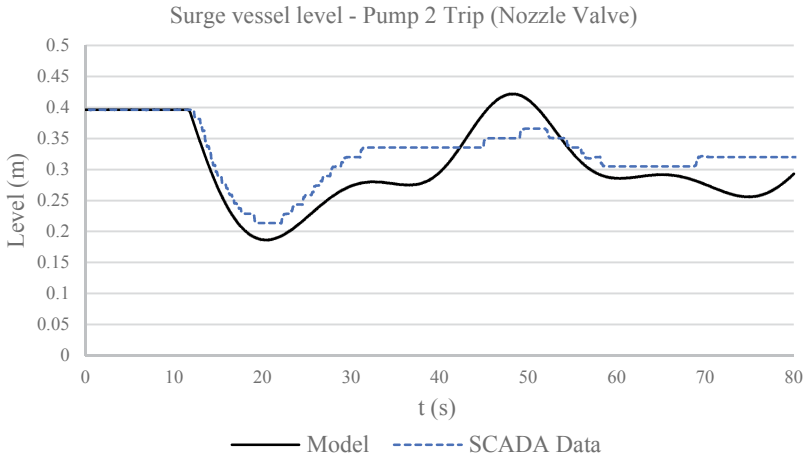

Figure 14. Modelled water level in the surge vessel vs. recorded level on the SCADA for nozzle check valve after trip.

6 CONCLUSIONS

The conclusion and general recommendations drawn from this study are the following:

The use of HFPT on model calibration is strongly recommended when analysing systems with high wavespeeds, short pipes and significant transmission and reflection phenomena.

The slam effect of a swing check valve originates a peak pressure almost 6 times larger ($P_{steady\ state}$+47 m) than the one from a nozzle check ($P_{steady\ state}$ +8 m) during the initial instant. The first and second peak pressures caused by the swing check valve slam (217,7 and 202,4 m) exceed instantly the maximum allowable pressure on the system, 20 bar (200 m), determined by the old surge vessel data-plate. On the other, the peak pressure with the nozzle check (177,8 m) is lower than the maximum pressure set before the pumping station revamping. The test data highlights the importance of a proper check valve selection to mitigate initial pressure peaks. In the light of the results, the water operator replaced the swing check valve installed on Pump 1 with a second nozzle check valve, Figure 15.

Dynamic performance data of check valves from Thorley and Ballun (6, 8), predict quite different reverse velocities than estimated from the measured pressures and modelling results for Tibidabo PS. There are numerous uncertainties when trying to compare modeling results to the measurement, among them non-uniform geometry and measured HFPT slightly downstream of the check valve exit where a converging tee exists and the diameter has changed from DN200 to DN300. Further, the nozzle check valve body is DN150 with a DN150 to 200 expansion fitting at the downstream flange. In the absence of reverse velocity information, the use of charts from both authors provide the best values for modellers. But modelers should use caution if their geometry is variable as is the case at Tibidabo.

The lack of information regarding the dynamic performance of check valves suggests that modellers assess different reverse velocity values to limit the slam impact on the system.

The Commercial 1D modelling tool used on the test (1), based on MOC, provides reliable results with good field data agreement after model calibration to the first pressure spike. The slow energy dissipation of the model explains the main differences observed with field data gathered with pressure transducers. The lack of information from GIS of operators and the need to simplify the models and associated calculation times are partially responsible for the observed differences. On the other hand, the use of steady friction formulas to compute transient head losses would also explain the pressure difference. This is not a major constraint for modellers for designing proper protection devices as energy decay does not affect the initial instant when pressure oscillation is larger.

Lozano, Bosch and Walters, 2018 (19) provides a link to all data, models, spreadsheets, specification sheets and raw measured data in this study.

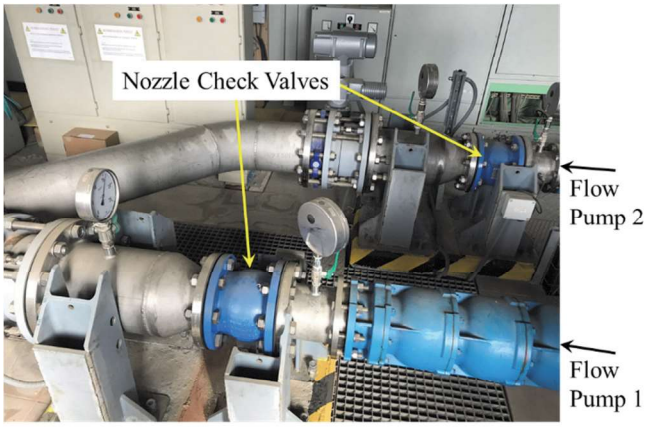

Figure 15. Final Tibidabo Pump Station configuration with nozzle check valves on both pump discharge lines

7 ACKNOWLEDGMENTS

Special thanks to *Aigües de Barcelona* and its technical staff for their contribution to the study and for making it possible and Javier Garrido from AQUATEC for his final contribution to the study. Thanks also to Stephanie Villars of Applied Flow Technology for creating hydraulic model diagrams (Figure 6) and work on model calibration, Dylan Witte of Purple Mountain Technology Group for assembling data for check valves and preparing Figure 8, and John Ballun of Val-Matic for providing the original report behind the Val-Matic check valve data from Reference 8.

8 REFERENCES

1. Applied Flow Technology, 2016, AFT Impulse 6, Colorado Springs, Colorado, USA.
2. Provoost, G.A., 1980, "The Dynamic Behavior of Non-Return Valves," *Proceedings of the 3rd International Conference on Pressure Surges*, BHRA, Canterbury, England, pp. 415-428.
3. Provoost, G.A., 1983, "A critical analysis to determine dynamic characteristics of non-return valves", *Proceedings of the 4th International Conference on Pressure Surges*, BHRA, Bath, England, Sept. 1983, pp. 275-286.

4. Thorley, A.R.D., 1983, “A critical analysis to determine dynamic characteristics of non-return valve Dynamic Response of Check Valves”, *Proceedings of the 4th International Conference on Pressure Surges*, BHRA, Bath, England, Sept. 1983, pp. 231-242.
5. Thorley, A.R.D., 1989, “Check Valve Behavior under Transient Flow Conditions, a State-of-the-Art Review,” *ASME Journal of Fluids Engineering*, ASME, Vol. 111, June 1989, pp. 178-183.
6. Thorley, A. R. D., 2004, Fluid Transients in Pipeline Systems, D. & L. George Ltd, Hertfordshire, England.
7. Val-Matic Valve and Manufacturing Corp., 2003, “Dynamic Characteristics of Check Valves”.
8. Ballun, J. V., 2007, “A methodology for predicting check valve slam”, *AWWA Journal,* 99(3):60-65, March 2007.
9. Liou, J. C. P. and Li, G, 2004, “Provoost's dynamic characteristic of check valves revisited”, *9th International Conference on Pressure Surges*, Chester, England, pp. 331-334.
10. Adriasola, J. M. and Rodríguez, B., 2014, “Early selection of check valve type considering the “slam” phenomenon”, *ASCE Pipelines 2014*, August 3-6, 2014, Portland, Oregon.
11. Marcinkiewicz, J., Adamkowski, A., Lewandowski, M. and Janicki, W., 2014, “EXPERIMENTAL INVESTIGATION OF DYNAMIC CHARACTERISTICS OF SWING AND TILTED DISC CHECK VALVES”, *Proceedings of the 2014 22nd International Conference on Nuclear Engineering ICONE22*, July 7-11, 2014, Prague, Czech Republic, ICONE22-30879.
12. Erhard brochure. www.erhard.de/frontend/project/popup_downloaddocuments.php?datei=3/389/media/leaflets/3/ERHARD_non_slam_nozzle_check_valve_EN.pdf
13. Wylie, E. B. and Streeter, V. L., 1993, *Fluid Transients in Systems*, Prentice Hall, Englewood Cliffs, NJ.
14. Chaudhry, M. H., 2014, *Applied Hydraulic Transients*, 3rd Ed., Springer, New York.
15. Bergant, A., Simpson, A. R. and Tijsseling, A. S., 2006, “Water hammer with column separation: A historical review”, *Journal of Fluids and Structures*, 22, 135-171.
16. Karney, W., Filion, Y. R. 2003. “Energy dissipation mechanisms in water distribution systems”. Proceedings of ASME, FEDSM’03, 4th ASME_JSME Joint Fluids Engineering Conference. Honolulu, Hawaii, USA, July 6-10, 2003.
17. Abreu, J. y Almeida, A.B. (2000) - "Pressure transient dissipative effects: a contribution for their computational prediction". Proc. 8th Int. Conf. on Pressure Surges and Fluid Transients, The Hague, The Netherlands. BHR Group Conf. Series, Publication No.39, pp.499-518.
18. Leite, P., Covas D. I. C., Ramos, H. M., Valente, J. T., Pacheco, M. M. 2012. “Evaluation of flow resistance in unsteady pipe flow: numerical developments and first experimental results”. Lisbon, Porto.
19. Lozano Solé, D., Bosch Segarra, R., and Walters, T. W., (2018), Auxiliary data files, http://www.aft.com/learning-center/technical-papers/surge-transients-due-to-check-valve-closure-in-a-municipal-water-pumping-station